IEEE Access
Multidisciplinary | Rapid Review | Open Access Journal

Received January 13, 2019, accepted January 21, 2019, date of publication January 25, 2019, date of current version February 14, 2019.

Digital Object Identifier 10.1109/ACCESS.2019.2895126

Rayleigh Fading Suppression in One-Dimensional Optical Scatters

SHENGTAO LIN[1], ZINAN WANG[1,2], (Senior Member, IEEE), JI XIONG[1], YUN FU[1], JIALIN JIANG[1], YUE WU[1], YONGXIANG CHEN[1], CHONGYU LU[1], AND YUNJIANG RAO[1], (Fellow, IEEE)

[1]Key Laboratory of Optical Fiber Sensing and Communications, University of Electronic Science and Technology of China, Chengdu 611731, China
[2]Center for Information Geoscience, University of Electronic Science and Technology of China, Chengdu 611731, China

Corresponding author: Zinan Wang (znwang@uestc.edu.cn)

This work was supported in part by the Natural Science Foundation of China under Grant 41527805 and Grant 61731006, in part by the Sichuan Youth Science and Technology Foundation under Grant 2016JQ0034, in part by the Guofang Keji Chuangxin Tequ, and in part by the 111 Project under Grant B14039.

ABSTRACT A highly coherent wave is favorable for applications in which phase retrieval is necessary, yet a high-coherence wave is prone to encounter Rayleigh fading phenomenon as it passes through a medium of random scatters. As an exemplary case, a phase-sensitive optical time-domain reflectometry (Φ-OTDR) utilizes the coherent interference of backscattering light along a fiber to achieve ultra-sensitive acoustic sensing, but sensing locations with fading will not be functional. Apart from the sensing domain, fading is also ubiquitous in optical imaging and wireless telecommunication, and therefore, it is of great interest. In this paper, we theoretically describe and experimentally verify how the fading phenomenon in one-dimensional (1-D) optical scatters will be suppressed with an arbitrary number of independent probing channels. We initially theoretically explained why fading would cause severe noise in the demodulated phase of Φ-OTDR; then, M-degree summation of incoherent scattered light-waves is studied for the purpose of eliminating fading. Finally, the enhancement and the fluctuation of retrieved phase signal-to-noise-ratio were analytically derived and experimentally verified. This paper provides a guideline for the fading elimination in 1-D optical scatters, and it also provides insight for optical imaging and wireless telecommunication.

INDEX TERMS Optical fiber sensors, phase-sensitive optical time-domain reflectometry, fading, Rayleigh channels, multiplexing.

I. INTRODUCTION

Fading is a ubiquitous phenomenon in the field of wireless telecommunication (three dimensions, 3-D), optical imaging (two dimensions) and distributed optical fiber sensing (one dimension, 1-D). Fading phenomenon is characterized by a random attenuation of the signal. The signals may be reflected by various surfaces and reach the receiver via different paths. The received information is the sum of all the signals from varieties of paths. When they interfere with each other and out of phase, the fading phenomenon appeared. Such a phenomenon may lead to temporary failure of communication, deterioration of image quality or degradation of the sensor's performance.

In order to comprehensively study fading phenomenon, reducing the number of dimensions of the problem might be a wise way. The related purpose of the optical imaging field is to obtain a speckle-free (without fading points) map with more emphasis on the intensity currently [1], and the effect of speckle on the retrieved phase could also be a significant issue, which is far from fully explored. On the other hand, phase-sensitive optical time-domain reflectometry (Φ-OTDR), which uses the randomly distributed Rayleigh scattering inside an optical fiber (1-D scatters) as the sensing mechanism, may be an ideal carrier [2].

Compared with optical imaging, Φ-OTDR focuses more on obtaining the phase information from the intensity traces. Furthermore, due to the maturity of the high-quality fiber manufacture process, there is no strong reflection point inside the fiber and the scattering elements are frozen. Particularly, each resolvable segment of the fiber contains large number of randomly distributed Rayleigh scatters, which sufficiently satisfies the central limit theorem. As a result, Φ-OTDR can be considered as special 1-D Rayleigh channels in analogy to the field of wireless telecommunication. The case is similar to

the propagation of radio signals in the heavily built-up urban environments (3-D) [3], but the external environment is more controllable for Φ-OTDR.

The fading phenomenon in Φ-OTDR comes from the randomly spatial non-uniform distribution of the refractive index [4]. Fading points (extremely low intensity backscattering points) are detrimental for obtaining external disturbance information in Φ-OTDR system. Reference [5] has explained that the retrieved phase signal-to-noise-ratio (SNR_ϕ) depends on intensities of the sampled points. At the fading points, the intensity noise will bring intolerably large noise after phase demodulation. That paper also gives an analytical formula for the mean value of SNR_ϕ. The fluctuation of SNR_ϕ was characterized by the coefficient of variation (C_V), which is as high as 0.8944 for traditional single frequency Φ-OTDR [6]. A similar definition exists in the field of optical imaging, namely speckle contrast, but it is used to describe intensity fluctuation.

In order to reduce fading points, a straightforward thought is to add M statistically independent field components (M degrees of freedom), such as orthogonal frequency division multiplexing (OFDM) [7] used in wireless telecommunication, multi-mode incoherent light [8] used in optical imaging and inner-pulse frequency-division method [9] used in distributed optical fiber sensing. For Φ-OTDR, Reference [10] discussed the rationality of using multi-frequency to eliminate fading phenomenon. The condition for two probe signals to be statistically independent is that their frequencies differ by at least the inverse pulse duration [11]. Since the backscattering signals is complex, it is not advisable to directly aggregate different frequency backscattering signals on the intensity, which causes phase mix-up. Reference [9] proposed rotated-vector-sum method to aggregate backscattering signals with four different frequencies, which is proved to be effective. Besides, the relationship between the number of aggregated frequencies and SNR_ϕ is shown in [12]. Based on the simulation results, the SNR_ϕ enhancement factor is closed to $\sqrt{M}$, which is similar to M averages on a single frequency intensity traces [13]. However, to the best of authors' knowledge, no one has theoretically studied the statistical regularity of SNR_ϕ after aggregating arbitrary degrees of freedom.

In this work, the fading problem in one-dimensional optical scatters has been studied in depth, using Φ-OTDR as the platform. Firstly, the effect of intensity noise on the demodulated absolute phase is derived, which is a completely different approach compared with previous literatures [5], [14]. Moreover, to embody the fading suppression after aggregating arbitrary degrees of freedom, a statistical model is elaborated: for intensity statistics, the amplitude distribution after aggregation is introduced and the decreasing of speckle contrast was observed from experiments; for retrieved phase statistics, the enhancement and the fluctuation of SNR_ϕ were also analytically derived, and the results were verified by the simulations and experiments.

This paper is organized as follows. Section II introduces the effect of intensity noise on the demodulated phase from the analytical aspect. Section III describes the effect of fading points reducing after aggregating arbitrary degrees of freedom. Particularly, Section III. A gives the mathematical results, including aggregated amplitude distribution, the enhancement of SNR_ϕ and the level of SNR_ϕ fluctuations; Section III. B describes the experimental and simulated details.

II. THE EFFECT OF INTENSITY NOISE ON THE DEMODULATED PHASE

In Φ-OTDR, the phase information is extracted from the intensity traces. The effect of intensity noise in the phase demodulation process should be considered first.

For the typical Φ-OTDR system (single-carrier-frequency, single-polarization pulses probing a single-mode fiber), the in-phase and quadrature outputs, i.e., i and q, can be represented by (1) [15].

$$\begin{cases} i(k,t) = A_{k,t}\cos\left[(\omega_s - \omega_{LO})\,t + \phi_{k,t}\right] + n_i(k,t) \\ q(k,t) = A_{k,t}\sin\left[(\omega_s - \omega_{LO})\,t + \phi_{k,t}\right] + n_q(k,t) \end{cases} \tag{1}$$

In (1), t stands for the fast time axis, indirectly representing the position of the fiber; k stands for the slow time axis, indicating the changes of the information obtained at the same point after each pulse; ω_s is the angular frequency of signals while ω_{LO} is the angular frequency of local oscillator light; $\phi_{k,t}$ is the phase changes caused by external disturbance; n_i and n_q represent uncorrelated Gaussian white noise with zero mean and the same variance σ_n^2. It should be noted that for conveniently exploring the phase noise caused by intensity noise on the phase demodulation process, only intensity noise is considered. The detected i and q outputs are coming from the superposition of numerous Rayleigh scattering. According to the central limit theorem, the distribution of them are asymptotically Gaussian distribution with zero mean and variance σ^2 [16]. Thus, the amplitude A of backscattering signals is Rayleigh distribution in the fast time axis. However, during a relatively short period, the amplitude in the slow time axis ($A_{k,t}\big|_{t=t'}$) can be deemed as invariant [4].

Generally, in the slow time axis, n_i and n_q are two linear independent quantities and follow the two-dimensional Gaussian distribution. For convenience, n_i and n_q are normalized, and the joint probability density of them is

$$P_{x,y}(x,y) = \frac{1}{2\pi\delta^2}\exp[-\frac{1}{2}(\frac{x^2}{\delta^2} + \frac{y^2}{\delta^2})] \tag{2}$$

where x and y are $n_i(k,t')/A(t')$ and $n_q(k,t')/A(t')$ respectively, and δ^2 is normalized variance of intensity noise (i.e., $\delta^2 = \sigma_n^2/A^2(t')$).

The intensity noise existed in i/q outputs can have impact on the demodulated phase signals, that is to say, the intensity noise transfers to phase noise after phase demodulation.

The phase noise can be expressed as:

$$\Delta\left(k,t'\right)=\arctan\left(\frac{\sin\Phi\left(k,t'\right)+\mathrm{x}}{\cos\Phi\left(k,t'\right)+\mathrm{y}}\right)-\Phi\left(k,t'\right) \quad (3)$$

where $\Phi(k,t')=(\omega_S-\omega_{LO})\,t'+\phi_{k,t'}$ is the sum of a constant and the phase change caused by the external disturbance. The similar case is common in the communication domain, and the distribution of phase information after adding Gaussian noise is described in [17]. Here, the probability density function (PDF) of phase noise Δ in Φ-OTDR can be obtained directly using a modified Jacobian determinant [18].

$$P_{\Delta}(\Delta)=\int_{-\infty}^{+\infty}P_{x,y}(x(y,\,\Delta),\,y)|\frac{\partial x}{\partial\Delta}|dy \quad (4)$$

where $x(y,\,\Delta)$ is available from the inverse function of (3) and $\frac{\partial x}{\partial\Delta}$ is the partial derivative of x to Δ. The calculation details are given in Appendix A and the result is shown in the first row of (5). Besides, when the normalized intensity noise δ^2 is extremely small, the distribution of $\Delta\left(k,t'\right)$ is concentrated near 0, i.e., $sin\Delta\sim\Delta$ and $\cos\Delta\sim1$. The equation of $P_{\Delta}(\Delta)$ can be further reduced.

$$\begin{aligned}P_{\Delta}(\Delta)&\approx\frac{1}{\sqrt{2\pi}\delta}\exp(-\frac{sin^2\Delta}{2\delta^2})\cos(\Delta)\\&\approx\frac{1}{\sqrt{2\pi}\delta}\exp(-\frac{\Delta^2}{2\delta^2})\end{aligned} \quad (5)$$

It should be noted that, the phase noise obeys Gaussian distribution approximatively, so the variance of the phase noise transferred from the intensity noise is about δ^2. In other words, in the case of low intensity noise (i.e., $A^2\gg\sigma_n^2$), the phase noise is inversely proportional to the intensity of backscattering signal. For low intensity signal comparing with noise, the linear relationship is not valid. However, it is certain that the extremely low intensity point will bring large phase noise and deteriorate the demodulated disturbance, which will cause the phenomenon of fading.

III. THE STATISTICAL REGULARITY OF RETRIEVED PHASE SNR$_\phi$

As mentioned in Section II, extremely low intensity backscattering points can cause fading phenomenon. The summation of arbitrary degrees of backscattering light-waves is benefit to reduce the fading points, thereby acquiring high-quality phase information. Here, the statistical methods, including analyzing the mean and the fluctuations of SNR_ϕ, are used to evaluate the changes of sensing performance.

A. THEORY

Due to the phase accumulation with the fiber length, it is necessary to use a differential process to obtain external disturbance. Thus, the value of SNR_ϕ is associated with backscatter power of two differential points, which is given by [5]

$$SNR_\phi=\frac{\sigma_\phi^2}{\sigma_n^2\left[1/A^2(t_1)+1/A^2(t_2)\right]} \quad (6)$$

where σ_ϕ^2 is the variance of external disturbance; t_1 and t_2 are the positions of two differential points. Therefore, the mean value and fluctuation level of SNR_ϕ are related to the amplitude distribution of two differential points.

Unlike direct intensity superposition [19], the aggregation of complex signals is related to the signal angle. When the signal angles are all the same, the stacking gain is maximum, which is the same as the amplitude summation. Therefore, in Φ-OTDR, the amplitude distribution for aggregated signals can be deemed as Rayleigh sum distribution. A relatively simple and widely used small argument approximation for obtaining Rayleigh sum PDF was described in [20]. Although this approximation is not perfect, the error has little effect on subsequent calculations and the expression is concise. Approximate equation of the Rayleigh sum PDF is:

$$f_R(s)=\frac{s^{2M-1}e^{-\frac{s^2}{Mb}}}{2^{M-1}b^M(M-1)!M^M} \quad (7)$$

where s is the sum of M statistically independent Rayleigh random signals, $(2M-1)!!=(2M-1)(2M-3)\cdots3\cdot1$, and $b=\frac{\sigma^2}{M}[(2M-1)!!]^{1/M}$. It is assumed that each signal has the same intensity, namely $\left\langle A_1^2\right\rangle=\left\langle A_2^2\right\rangle=\cdots=\left\langle A_M^2\right\rangle=2\sigma^2$. Taking into account the intensity noise on each frequency trace, the aggregated intensity noise becomes $\sigma_{n,M}^2=M\sigma_n^2$. Thus, the mean SNR_ϕ can be calculated using software Mathematica.

$$\begin{aligned}\mu\left(SNR_\phi\right)&=\iint\left[f_R\left(A(t_1)\right)\cdot SNR_\phi\cdot f_R\left(A(t_2)\right)\right]dA\left(t_1\right)dA(t_2)\\&=\frac{2M\left((2M-1)!!\right)^{1/M}}{(1+2M)}\frac{\sigma^2\sigma_\phi^2}{\sigma_n^2}\\&=\frac{2}{3}K^2\sigma_\phi^2SNR_{intensity}\end{aligned} \quad (8)$$

where $SNR_{intensity}\equiv\sigma^2/\sigma_n^2$ is intensity SNR for single frequency backscattering signal and the K is the enhancement factor (i.e., gain) of SNR_ϕ. However, the expression of gain K is very complicated with double factorial. In order to simplify the expression, Stirling's approximation [21] is adopted, which is a good formula for accurately estimating factorials. The gain K can be approximated as:

$$K^2=\frac{3M\left((2M-1)!!\right)^{1/M}}{(2M+1)}\approx\frac{6M^2}{(2M+1)\,e} \quad (9)$$

where e is the mathematical constant. The simplified process is given in Appendix B. Notably, for larger value of M, gain K approaches to $\sqrt{3M/e}\approx1.05\sqrt{M}$.

In order to reflect the effect of reducing fading points, the level of SNR_ϕ fluctuations can also be an important indicator. However, the statistical distribution of SNR_ϕ is particularly wide, and it is unsuitable to use the variance to measure the SNR_ϕ fluctuation. Using the C_V to measure it may be more lucid, which can be expressed as

$$C_V\left(SNR_\phi\right)=\frac{\sigma\left(SNR_\phi\right)}{\mu\left(SNR_\phi\right)}=\sqrt{\frac{2M^2+5M+1}{4M^3+6M^2}} \quad (10)$$

where $\sigma\left(SNR_\phi\right)$ is the standard deviation of SNR_ϕ. $\sigma(SNR_\phi) \equiv \sqrt{\mu\left(SNR_\phi^2\right) - \mu^2\left(SNR_\phi\right)}$, where $\mu\left(SNR_\phi^2\right)$ can be obtained with the same method as (8).

It can be found from (9) and (10), with the increase of aggregated number M, the mean value of SNR_ϕ increases linearly and the level of fluctuation decreases exponentially.

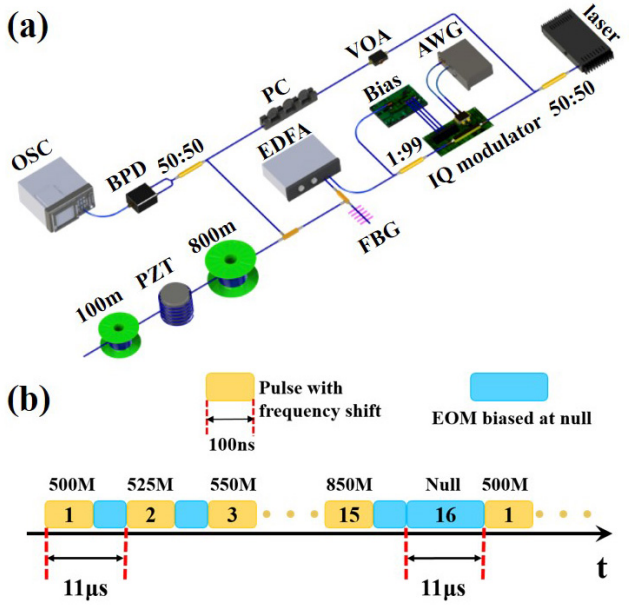

FIGURE 1. Experimental setup of Φ-OTDR. (a) AWG, arbitrary waveform generator; VOA, variable optical attenuator; EDFA, Erbium-doped fiber amplifier; FBG, fiber Bragg grating; PC, polarization controller. (b) 15 groups of differential frequency-shift pulse generated by IQ modulator and the 16th group is to measure the intensity noise.

B. EXPERIMENTS AND SIMULATIONS

The experiment setup shown in Fig. 1 is to verify the impact of aggregating M degrees of freedom on eliminating fading. An ultra-narrow linewidth laser with small phase noise is used, and the output is split into two branches by a 50:50 coupler, namely the signal branch and the local oscillator (LO) branch. The signal branch is modulated by an IQ modulator, generated frequency shift pulse with 100 ns width. After amplified by EDFA, the pulse is injected into the sensing fiber through a circulator. A piezoelectric ceramic transducer (PZT) wrapped with 12.7 m fiber is inserted between the 800 m and 100 m fiber sections, applied with 100 Hz sinusoidal perturbation. The Rayleigh scattering signal is injected into 50:50 coupler together with the LO. The outputs of 50:50 coupler are converted into electrical intensity signals by a 1.6 GHz balanced photo-detector (BPD), and then sampled by an oscilloscope (OSC) with 2 GS/s sampling rate. The initial frequency shift of the pulse is 500 MHz. After a round-trip time of the pulse in the fiber, another pulse with a larger frequency shift is applied, as shown in Fig. 1(b). The frequency shift interval is 25 MHz to ensure that each group of trace statistically independent. There are 15 groups of pulses with different frequency shifting from 500 MHz to 850 MHz, and another round trip time is reserved for measuring the intensity noise, during which the IQ modulator stays at the null point. This method helps detect the leakage of light from the IQ modulator and the noise contributed by the EDFA.

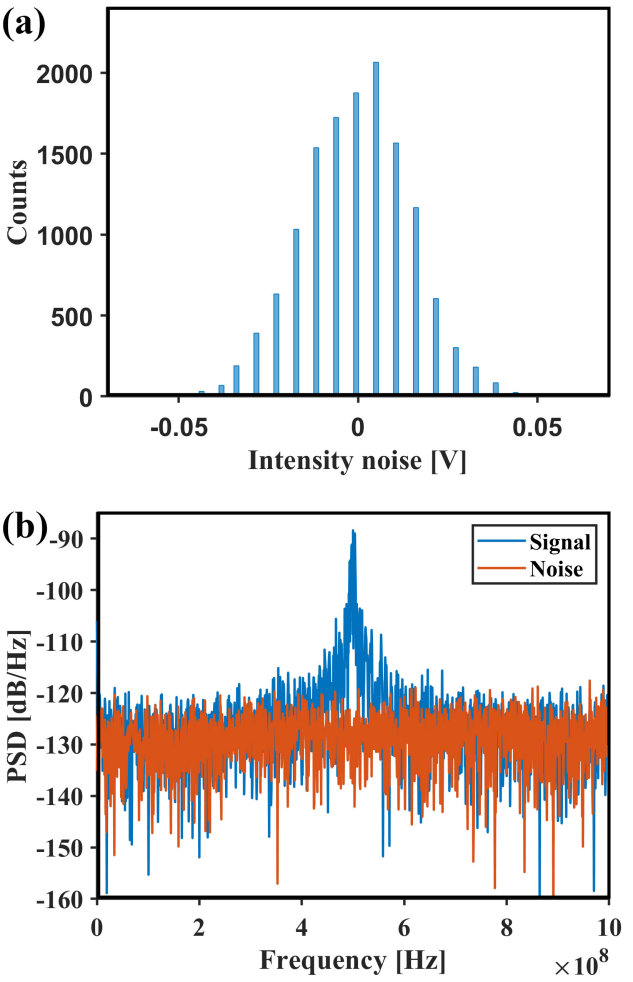

FIGURE 2. Statistical results of intensity noise. (a) The probability distribution. (b) PSD (blue line: signal; read line: noise).

From the experimental results, the main noise of the system comes from the detector and the local oscillator. The PDF and power spectral density (PSD) of the real part of the signal noise are shown in Fig. 2(a) and (b), respectively. The probability distribution of noise is approximately Gaussian, and the gap in it is caused by insufficient vertical resolution of the oscilloscope. In addition, the PSD of the noise is flat, so it can be considered as Gaussian white noise. The PSD of measured noise coincides with the background noise of the signal PSD, which indicates that measuring intensity noise in this way is reasonable.

In order to effectively aggregate scattered signals with different carrier frequencies and verify the aforementioned theoretical results, phase alignment is required. We used rotated-vector-sum method to aggregate each backscattering signals [9]. The method rotates the phase of each frequency backscattering signals to be aligned, ensuring the maximum intensity superposition. The normalized backscattering

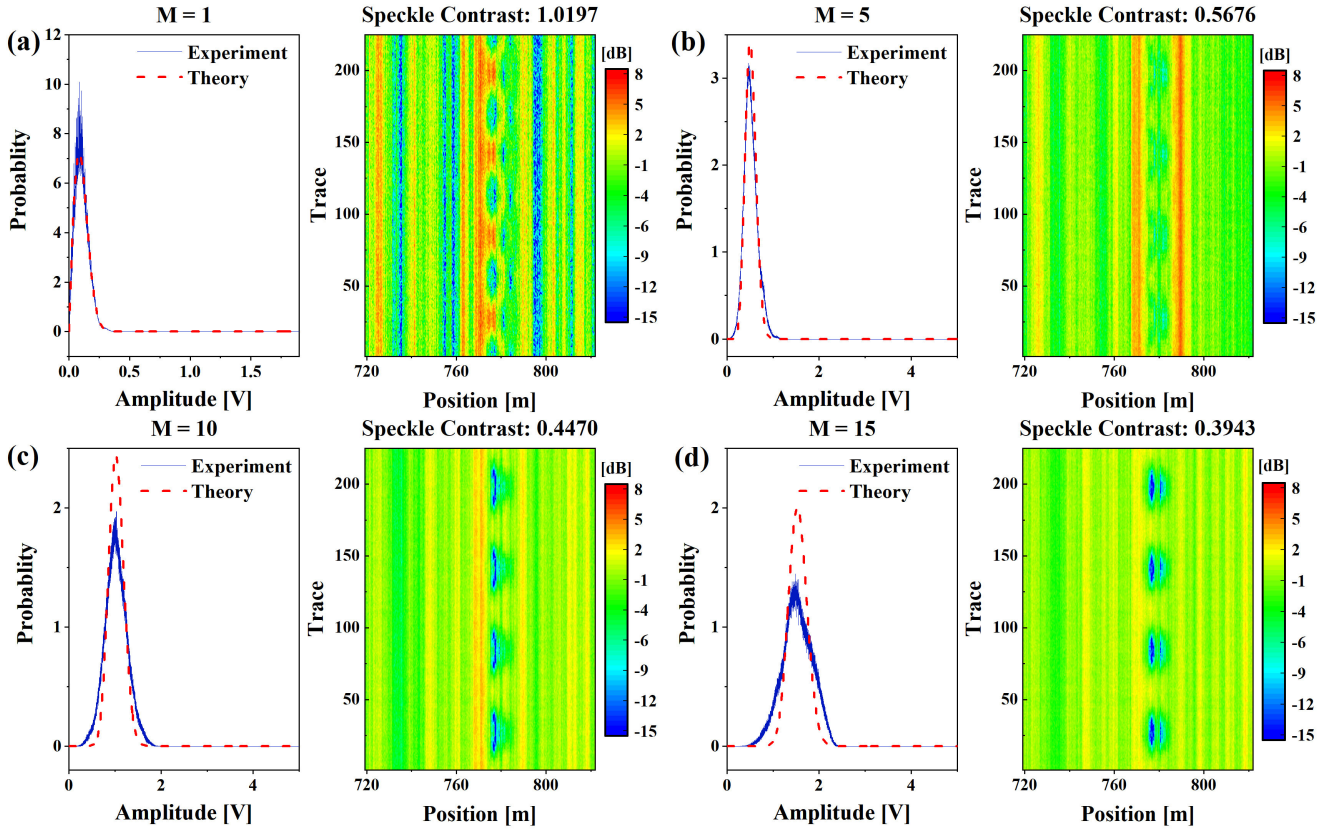

FIGURE 3. The amplitude distribution (left side) and normalized backscattering amplitude profile (right side) after aggregating M uncorrelated signals.

amplitude profile after aggregation was shown in Fig. 3 (right-hand side of each sub-figure). In the fast time axis (''Position'' axis), as the number of superimposed frequencies increases, the intensity fluctuations gradually decrease. In the slow time axis (''Trace'' axis), the intensity fluctuations are small except for the disturbed region, which is related to the intensity modulation from the external disturbance.

In accordance to the aforementioned assumption (the amplitude is invariant in the slow time axis), the two differential points must be away from the disturbed region. The speckle contrast from each image was calculated as $\sigma_I/\langle I\rangle$, where σ_I is the standard deviation of the intensity and $\langle I\rangle$ is the mean intensity. After superimposing 15 degrees of freedom in Φ-OTDR, the speckle contrast decreased from 1.02 to 0.39.

It is worth noting that the relationship between intensity changes and external disturbance is far from linear; therefore, the variation magnitude in intensity traces could not represent the magnitude of demodulated disturbance. The essence of fading suppression is to eliminate the low-level points in the intensity traces, which is the basis for acquiring high-quality phase information along the whole sensing fiber, that is to say, the speckle contrast reflects the possibility of high-quality phase demodulation.

Besides, the amplitude distribution after aggregation is plotted in Fig. 3 (left-hand side of each sub-figure). The theoretical curve was based on (7). The value of σ^2 in it was

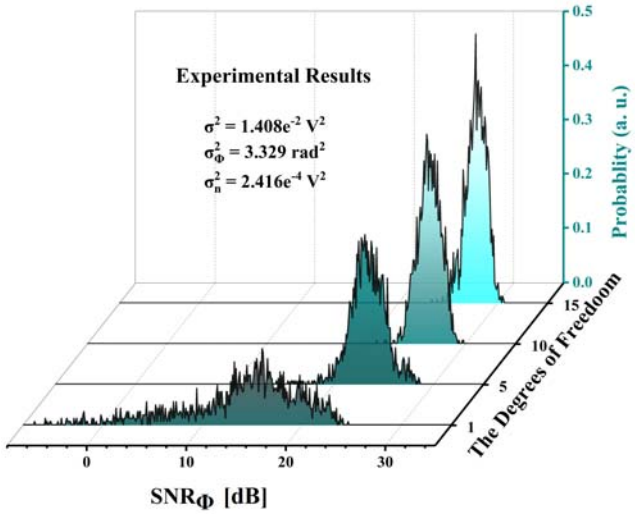

FIGURE 4. M degrees of freedom v.s. the PDF of SNR_ϕ from experimental results.

taken from the experiment ($\sigma^2 = 0.014076\ V^2$). In Fig. 3, experimental and theoretical results will have a few differences after aggregating more than 5 degrees of freedom. This can be attributed to the fact that the gain spectrum of detector is not flat, then the strength of each scattered signal will be slightly different, as a result the PDF of the amplitude gradually becomes broadened. Therefore, it can be expected

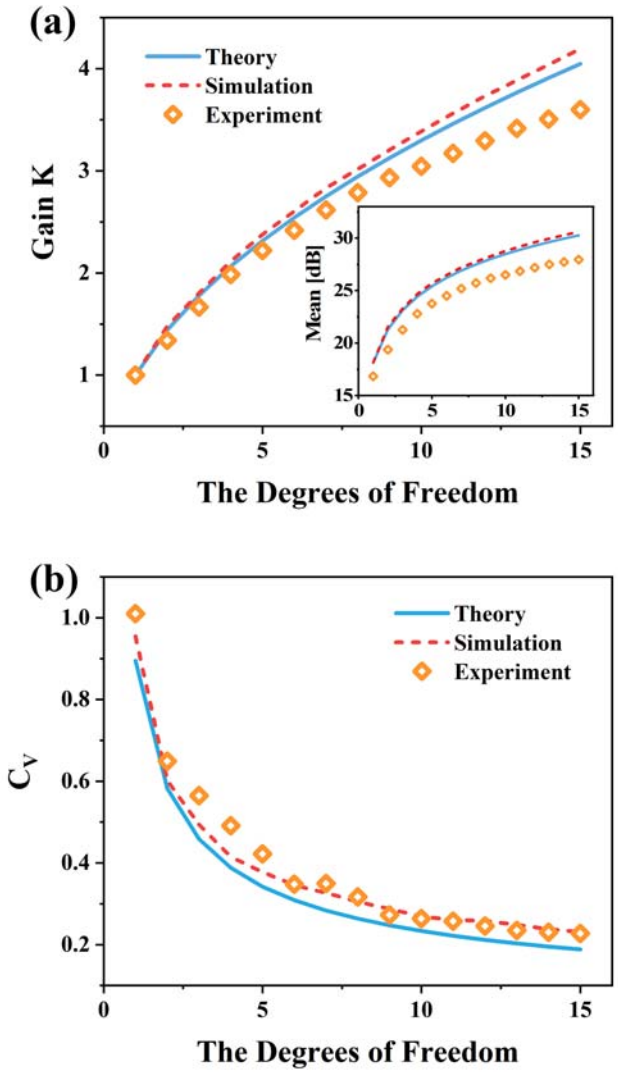

FIGURE 5. (a) Gain K, mean (inset in (a)) and (b) coefficient of variation of SNR_ϕ v.s. M degrees of freedom.

that the value of experimental C_V will be slightly higher than the theoretical value.

To obtain the mean and the C_V of SNR_ϕ, the measurements were repeated over 20 times. The gauge length is set to be 40 m, which is much larger than the PZT disturbance length (12.7 m). It ensures that the two differential points can be located on both sides of the disturbed region, away from the unstable intensity area shown in Fig. 3. Besides, the longer gauge length allows us to get more than a hundred sets of PZT disturbance signals after one measurement, which is conducive to acquiring large amounts of SNR_ϕ data. The distribution of SNR_ϕ is plotted in Fig. 4. The parameters in (8), obtained from experiments, are also listed inside the figure. As the degrees of freedom increases, the distribution of SNR_ϕ became sharper and average SNR_ϕ increased.

A set of simulations is also used to verify the correctness of the theory. The fiber parameters are based on [22]. The scatters in the fiber are randomly distributed. The perturbation of the fiber is introduced by changing the separation among the affected scatters. Besides, the intensity noise is fixed in each simulation and is consistent with the $SNR_{intensity}$ in the experiment. For statistic study, the positions of the scattering elements are considered to be fixed in the same simulation, but they are completely different among the simulations.

The illustration in Fig. 5(a) shows the results of mean value of SNR_ϕ obtained by theory (blue), simulations (red) and experiments (yellow). Mean value of SNR_ϕ from experiments are lower than the theory and simulation, which may come from the polarization effects and Hilbert transform error in this system. However, the experimental results of gain K at the low degrees of freedom ($M \leq 5$) is closed to theoretical and emulational results (plotted in Fig. 5(a)). The subsequent deviation of the gain K (when $M > 5$) is related to non-flat gain spectrum of the detector. In addition, the changes of C_V value have been drawn in Fig. 5(b). Since the scattering elements are completely different in each simulation but the intensity noise is fixed, it results in different $SNR_{intensity}$ in each simulation, which is more obvious in experiments. But the fluctuation range of the $SNR_{intensity}$ is only 0.5 dB in the experiments, which is much lower than the SNR_ϕ fluctuation. Due to slight fluctuation of $SNR_{intensity}$ results the experimental and emulational C_V value are slightly larger than the theoretical value, but the tendency is basically the same.

IV. CONCLUSIONS

We studied the fading phenomenon in one-dimensional optical scatters with statistical analysis. The reason of occurring fading phenomenon at low intensity point was mathematically explained. Moreover, the quantitative relationship between the degree of freedom and fading phenomenon was analyzed in detail. This work provides a lucid guideline for the choice of the degree of freedom to eliminate fading in 1-D optical scatters, which is crucial of fiber sensing based on Rayleigh scattering, and it would be also beneficial for optical imaging and wireless telecommunication domains.

APPENDIX A
THE APPROXIMATION OF PHASE NOISE PROBABILITY DENSITY FUNCTION

In (4), $x(y, \Delta)$ and $\frac{\partial x}{\partial \Delta}$ can be expressed as:

$$\begin{cases} x = \tan(\Delta + \Phi) \cdot (\cos\Phi + y) - \sin\Phi \\ \dfrac{\partial x}{\partial \Delta} = \dfrac{\cos\Phi + y}{\cos^2(\Delta + \Phi)} \end{cases} \tag{11}$$

Substituting (11) into (4) can obtain

$$\begin{aligned} P_\Delta(\Delta) &= \int_{-\infty}^{+\infty} f(x(y,\Delta), y) \left| \frac{\partial x}{\partial \Delta} \right| dy \\ &= \int_{-\infty}^{+\infty} \frac{1}{2\pi\delta^2} \\ &\quad \cdot \exp\{-\frac{[\tan(\Delta+\Phi)\cdot(\cos\phi + y) - \sin\Phi]^2 + y^2}{2\delta^2}\} \\ &\quad \cdot \left| \frac{\cos\Phi + y}{\cos^2(\Delta+\Phi)} \right| dy \end{aligned} \tag{12}$$

In order to obtain integral result, the error function $(erf\left(\sqrt{c}z\right) \equiv 1 - 2\sqrt{\frac{c}{\pi}}\int_z^{+\infty} e^{-c\cdot t^2}dt$, where c and z are an arbitrary constant) is also introduced.

$$P_\Delta(\Delta) = \frac{1}{\pi}\exp\left(-\frac{1}{2\delta^2}\right) - \exp\left(\frac{sin^2\Delta}{-2\delta^2}\right) \cdot \frac{\cos(\Delta+\Phi)}{|\cos(\Delta+\Phi)|}\cos(\Delta)\frac{erf\left[-\frac{\cos(\Delta)|\cos(\Delta+\Phi)|}{\delta\sqrt{2}\cos(\Delta+\Phi)}\right]}{\delta\sqrt{2\pi}} \tag{13}$$

The approximation of error function can be represented by the Q-function [23], which is expressed as:

$$\begin{aligned} erf\left(\frac{z}{\sqrt{2}}\right) &= 1 - 2Q(z) \\ Q(z) &\approx \frac{\left(1 - e^{-1.4z}\right)e^{-\frac{z^2}{2}}}{1.135\sqrt{2\pi}z},\ z > 0 \\ Q(z) &= 1 - Q(-z) \end{aligned} \tag{14}$$

In addition, considering that the signal strength in the Φ-OTDR system is much larger than the noise, the value of $\cos(\Delta)$ can be considered to be greater than 0. As a rsesult, whether the value of $\cos(\Delta+\Phi)$ is greater than 0 or less, (13) can be reduced to the same equation shown in (15)

$$\begin{aligned} P_\Delta \approx\ & \frac{0.135}{\pi}\exp\left(-\frac{1}{2\delta^2}\right) \\ & + \frac{1}{\sqrt{2\pi}\delta}\exp\left(-\frac{sin^2\Delta}{2\delta^2}\right)\cos(\Delta) \\ & + \frac{1}{1.135\pi}\exp\left(-\frac{1}{2\delta^2} - 1.4\frac{\cos(\Delta)}{\delta}\right)\ for\ |\Delta| < \frac{\pi}{2} \end{aligned} \tag{15}$$

It is worth noting that δ is a small quantity and greater than 0. Thus, the first and last items in (15) are much smaller than the second one and can be ignored. The final result is given in the first row of (5).

APPENDIX B
THE APPROXIMATION OF GAIN *K*

The double factorial in (9) can be changed to a single factorial.

$$(2M-1)!! = \frac{(2M)!}{2^M M!} \tag{16}$$

In addition, the logarithmic form of gain K, can be expressed as:

$$\ln\left(K^2\right) = \ln\left[\frac{3M}{2(1+2M)}\right] + \frac{1}{M}\ln[(2M)!] - \frac{1}{M}\ln(M!) \tag{17}$$

Using Stirling's approximation $(\ln(n!) \approx n\ln(n) - n)$, the (17) can be reduced to

$$\ln\left(K^2\right) \approx \ln\left[\frac{6M^2}{2M+1}\right] - 1 \tag{18}$$

ACKNOWLEDGMENTS

The authors would like to thank Anderson S. L. Gomes in Universidade Federal de Pernambuco for helpful discussions.

REFERENCES

[1] N. Bender, H. Yılmaz, Y. Bromberg, and H. Cao, "Customizing speckle intensity statistics," *Optica*, vol. 5, no. 5, pp. 595–600, May 2018.
[2] H. F. Martins, K. Shi, B. C. Thomsen, S. Martin-Lopez, M. Gonzalez-Herraez, and S. J. Savory, "Real time dynamic strain monitoring of optical links using the backreflection of live PSK data," *Opt. Express*, vol. 24, no. 19, pp. 22303–22318, Sep. 2016.
[3] B. Sklar, "Rayleigh fading channels in mobile digital communication systems. I. Characterization," *IEEE Commun. Mag.*, vol. 35, no. 7, pp. 90–100, Jul. 1997.
[4] A. H. Hartog, *An Introduction to Distributed Optical Fibre Sensors*, 1st ed. Boca Raton, FL, USA: CRC Press, 2017.
[5] H. Gabai and A. Eyal, "On the sensitivity of distributed acoustic sensing," *Opt. Lett.*, vol. 41, no. 24, pp. 5648–5651, Dec. 2016.
[6] A. Eyal, H. Gabai, and I. Shpatz, "Distributed acoustic sensing: how to make the best out of the Rayleigh-backscattered energy?" in *Proc. 25th Int. Conf. Opt. Fiber Sensors*, Apr. 2017, pp. 1–4.
[7] A. Goldsmith, *Wireless Communications*. New York, NY, USA: Cambridge Univ. Press, 2005.
[8] B. Redding, M. A. Choma, and H. Cao, "Speckle-free laser imaging using random laser illumination," *Nature Photon.*, vol. 6, pp. 355–359, Apr. 2012.
[9] D. Chen, Q. Liu, and Z. He, "Phase-detection distributed fiber-optic vibration sensor without fading-noise based on time-gated digital OFDR," *Opt. Express*, vol. 25, no. 7, pp. 8315–8325, Mar. 2017.
[10] J. Zhou, Z. Pan, Q. Ye, H. Cai, R. Qu, and Z. Fang, "Characteristics and explanations of interference fading of a Φ-OTDR with a multi-frequency source," *J. Lightw. Technol.*, vol. 31, no. 17, pp. 2947–2954, Sep. 1, 2013.
[11] M. D. Mermelstein, R. Posey, G. A. Johnson, and S. T. Vohra, "Rayleigh scattering optical frequency correlation in a single-mode optical fiber," *Opt. Lett.*, vol. 26, no. 2, pp. 58–60, Jan. 2001.
[12] A. Hartog *et al.*, "The use of multi-frequency acquisition to significantly improve the quality of fibre-optic-distributed vibration sensing," *Geophys. Prospecting*, vol. 66, no. S1, pp. 192–202, Mar. 2018.
[13] Z. Wang *et al.*, "Distributed acoustic sensing based on pulse-coding phase-sensitive OTDR," *IEEE Internet Things J.*, to be published, doi: 10.1109/JIOT.2018.2869474.
[14] G. Yang, X. Fan, S. Wang, B. Wang, Q. Liu, and Z. He, "Long-range distributed vibration sensing based on phase extraction from phase-sensitive OTDR," *IEEE Photon. J.*, vol. 8, no. 3, Jun. 2016, Art. no. 6802412.
[15] Z. Wang *et al.*, "Coherent Φ-OTDR based on I/Q demodulation and homodyne detection," *Opt. Express*, vol. 24, no. 2, pp. 853–858, Jan. 2016.
[16] P. Healey, "Statistics of Rayleigh backscatter from a single-mode fiber," *IEEE Trans. Commun.*, vol. 35, no. 2, pp. 210–214, Feb. 1987.
[17] R. N. McDonough and A. D. Whalen, *Detection of Signals in Noise*, 2nd ed. New York, NY, USA: Academic, 1995.
[18] MIT OpenCourseWare. (2008). *Derived Distributions*. [Online]. Available: https://ocw.mit.edu/courses/electrical-engineering-and-computer-science/6-436j-fundamentals-of-probability-fall-2008/lecture-notes/MIT6_436JF08_lec10.pdf
[19] K. Shimizu, T. Horiguchi, and Y. Koyamada, "Characteristics and reduction of coherent fading noise in Rayleigh backscattering measurement for optical fibers and components," *J. Lightw. Technol.*, vol. 10, no. 7, pp. 982–987, Jul. 1992.
[20] N. C. Beaulieu, "An infinite series for the computation of the complementary probability distribution function of a sum of independent random variables and its application to the sum of Rayleigh random variables," *IEEE Trans. Commun.*, vol. 38, no. 9, pp. 1463–1474, Sep. 1990.
[21] J. Dutka, "The early history of the factorial function," *Arch. Hist. Exact Sci.*, vol. 43, no. 3, pp. 225–249, Nov. 1990.
[22] A. Masoudi and T. P. Newson, "Analysis of distributed optical fibre acoustic sensors through numerical modelling," *Opt. Express*, vol. 25, no. 25, pp. 32021–32040, Dec. 2017. [Online]. Available: http://www.opticsexpress.org/abstract.cfm?URI=oe-25-25-32021
[23] G. K. Karagiannidis and A. S. Lioumpas, "An improved approximation for the Gaussian Q-function," *IEEE Commun. Lett.*, vol. 11, no. 8, pp. 644–646, Aug. 2007.

SHENGTAO LIN received the B.S. degree from Northeastern University, in 2017. He is currently pursuing the master's degree in optical engineering with the Key Laboratory of Optical Fiber Sensing and Communications (Education Ministry of China), University of Electronic Science and Technology of China, Chengdu, China. His current research interests include random fiber lasers and distributed fiber optic sensing.

ZINAN WANG received the Ph.D. degree from the Beijing University of Posts and Telecommunications, China, in 2009. From 2007 to 2009, he was with Alcatel-Lucent Bell Labs as a Visiting Student. He was with Cornell University, as a Postdoctoral Research Associate, from 2009 to 2010. He joined the University of Electronic Science and Technology of China, in 2010, and became a Full Professor, in 2015. He has published over 130 papers in international journals and conference proceedings, and he holds 16 Chinese patents and 2 U.S. patents. His research interests include distributed fiber sensing and nonlinear fiber optics. He is a Senior Member of the IEEE and OSA. He has given over 15 invited talks at international conferences, and he served as a TPC Member for a number of conferences. His research was highlighted in Optics in 2014 by OSA Optics and Photonics News. He was a recipient of the IOP Publishing Top Cited Author Award, China, in 2018. He is an Associate Editor of the IEEE Photonics Technology Letters and the IEEE Access.

JI XIONG received the B.S. degree from the Wuhan University of Technology, in 2016. He is currently pursuing the Ph.D. degree in optical engineering with the Key Laboratory of Optical Fiber Sensing and Communications (Education Ministry of China), University of Electronic Science and Technology of China, Chengdu, China. His current research interests include distributed fiber optic sensing and optical signal processing.

YUN FU received the B.S. degree from the University of Electronic Science and Technology of China, Chengdu, China, in 2015, where she is currently pursuing the Ph.D. degree in optical engineering with the Key Laboratory of Optical Fiber Sensing and Communications (Education Ministry of China). Her current research interests include distributed fiber optic sensing and nonlinear fiber optics.

JIALIN JIANG received the B.S. degree from the Nanjing University of Science and Technology, in 2017. He is currently pursuing the Ph.D. degree in optical engineering with the Key Laboratory of Optical Fiber Sensing and Communications (Education Ministry of China), University of Electronic Science and Technology of China, Chengdu, China. His current research interest includes distributed fiber optic sensing.

YUE WU received the B.S. degree from the Nanjing University of Science and Technology, in 2017. She is currently pursuing the master's degree in optical engineering with the Key Laboratory of Optical Fiber Sensing and Communications (Education Ministry of China), University of Electronic Science and Technology of China, Chengdu, China. Her current research interests include distributed fiber optic sensing and nonlinear fiber optics.

YONGXIANG CHEN received the B.S. degree from the Changchun University of Science and Technology, in 2017. She is currently pursuing the master's degree in optical engineering with the Key Laboratory of Optical Fiber Sensing and Communications (Education Ministry of China), University of Electronic Science and Technology of China, Chengdu, China. Her current research interests include distributed fiber optic sensing and nonlinear fiber optics.

CHONGYU LU received the B.S. degree from the Southwest University of Science and Technology, in 2017. He is currently pursuing the master's degree in optical engineering with the Key Laboratory of Optical Fiber Sensing and Communications (Education Ministry of China), University of Electronic Science and Technology of China, Chengdu, China. His current research interests include distributed fiber optic sensing and nonlinear fiber optics.

YUNJIANG RAO received the Ph.D. degree in optoelectronic engineering from Chongqing University, Chongqing, China, in 1990. He joined the Electric and Electronic Engineering Department, Strathclyde University, U.K., as a Postdoctoral Research Fellow, from 1991 to 1992, and the Applied Optics Group, Physics Department, Kent University, U.K., as a Research Fellow and, then, a Senior Research Fellow, from 1992 to 1999. From 1999 to 2004, he was a Chang-Jiang Chair Professor with Chongqing University. Since 2004, he has been a Chang-Jiang Chair Professor with the University of Electronic Science and Technology of China, where he is currently the Director of the Key Laboratory of Optical Fiber Sensing and Communications (Ministry of Education). His research interests include fiber-optic sensors and devices. He is a Fellow of the IEEE, OSA, and SPIE.